# COMPARATIVE ANALYSIS OF DIFFERENT INVERTERS AND CONTROLLERS TO INVESTIGATE PERFORMANCE OF ELECTROSURGICAL GENERATORS UNDER VARIABLE TISSUE IMPEDANCE

***Ali Jafer Mahdi****
Department of Scientific Affairs, Al-Zahraa University for Women
56001 Karbala, Iraq
Department of Electrical and Electronic Engineering, University of Kerbala
Karbala 56001, Iraq, ali.j.mahdi@alzahraa.edu.iq
https://orcid.org/0000-0002-0162-4064

***Hussban Abood Saber***
Al-Safwa University College
56001 Karbala, Iraq, hussban.as@alsafwa.edu.iq
https://orcid.org/0000-0002-7442-5381

***Ali Mohammed Ridha***
Department Medical Instrumentation Techniques Eng., Al-Hussain University College
56001 Karbala, Iraq
College of Medicine, University of Al-Ameed
56001 Karbala, Iraq, ali.mohammed@huciraq.edu.iq
https://orcid.org/0000-0002-4813-3174

***Mohammed Jamal Mohammed***
College of Medicine, University of Al-Ameed
56001 Karbala, Iraq, eng.mohammed.j@alameed.edu.iq
https://orcid.org/0009-0000-1019-3123

*Article history: Received 16 April 2023, Received in revised form 10 May 2023, Accepted 10 May 2023, Available online 11 May 2023.*

**Highlight**
Reduction of heat dissipation and total harmonic distortion of electrosurgery generators by using multilevel inverters and fractional order PID.

**Abstract**
Electrosurgical generators (ESGs) are currently the most widely used surgical technology for clinical operations. The main disadvantage of ESGs is their output power is irregular due to the variable tissue impedance. The heat dissipation caused by the high amount of thermal energy generated leads to medical complications for both patient and surgeon. In this research, various inverter topologies and power controllers are investigated to specify the best structure that ensures best performance. The type of inverter topologies investigated are three level and five level, while the PID structures investigated are integer order (IO-PID) and fractional order (FO-PID). The simulation results indicate that FO-PID with five level inverters is better than IO-PID with three level inverters in terms of minimum heat dissipation rate and THD of the output voltage and current.

**Keywords**
electrosurgical generator; tissue impedance; multilevel inverter; integer order-PID; fractional order-PID.

## Introduction
Several centuries ago, heat was used to halt bleeding, and as technology evolved, a number of devices were invented that employ electrical energy to control bleeding and heal tissues. Modern electrosurgery is now one of the most extensively used surgical procedures [1]. Electrosurgery uses high-frequency electric currents to cut and dry target tissue (radio frequencies). This approach is used to achieve clinical outcomes with less blood loss and less time than typical operations [2]. Electrosurgery works by sending a high-frequency electric current through a conductor to the target tissues, where it is transformed into heat energy. The electrosurgical functions of cutting, coagulation, and drying are dependent on the kind of current wave, current density, tissue conductivity, electrode size, and time [3,4]. The ESG sends electrical energy to the tissues via electrodes

(monopolar and bipolar). The difference between the two varieties lies in the positioning of the active and return electrodes. In the monopolar, the active electrode connects to the generator to provide current to the tissues, while the return electrode connects to one region of the patient's body to send current back to the generator. In a bipolar electrode, the active and neutral electrodes of a bipolar electrode are close together, and the electric current flows via one of them, returning to the generator through the other, without going through the patient [5]. Most of the 230 million surgical procedures performed worldwide each year rely on electrical energy, which benefits both the patient and the medical team by speeding up cutting tissues and reducing medical team effort [6]. However, the irregular output power and high heat dissipation of ESG units can lead to several medical complications, including:

- Burns both the patient and the surgeon if the device is not properly controlled or if the electrodes are in contact with the patient's skin for an extended period. These burns can range from superficial skin burns to deeper tissue damage.
- The high heat generated by ESG units can cause tissue damage beyond the intended surgical site, leading to unintended injuries and complications.
- ESG units can cause involuntary muscle contractions and nerve stimulation.
- ESG units can produce smoke and fumes that can be harmful to both the patient and the surgical, which leads to respiratory problems, such as eye irritation.

The reason for this is due to vary the ESG's load (vital tissues), which, the tissue's structure and qualities, that are present in the form of impedance. This change in load causes a change in the ESG's output power directed at the target part, which does not match the power parameters specified by the specialist medical team to achieve the desired clinical effects [7]. As a result, it was necessary to find appropriate solutions to this problem, and the most optimal and appropriate solution, based on the findings of the studies in this field, was to develop an intelligent control system that would regulate the generator's output power independently of the medical team.

Many studies applied several control methods and compared them to find the best performing ESG. Perhaps some studies are still based on studying this problem, whose goal is to obtain the best performing ESG, as shown in [7–9]. These studies did not address this issue, which is reflected in the thermal effects of the generator, even if they addressed the issue of changing the ESG's output power due to changes in tissue impedance. Thermal diffusion is another issue that electrosurgical techniques address. Thermal damage is one of the most dangerous concerns in electrosurgical treatments, causing burns to the subject tissues during surgery or complications following surgery, some of which are serious enough to cause patient death. When studying this problem to find appropriate solutions. The type of biological tissue undergoing surgery, the distance between the tissue and the active electrode, the position of the returning electrode, the position of the operating cable, the properties of steam and gas, and the type of tool used to perform surgery are all factors that contribute to the complexity of the problem [10]. Several research studies have studied the problem and developed solutions. In [10], the researcher proposed using thermometric sensors to limit or eliminate thermal spread, which he demonstrated using a piece of chicken meat. In [11], the researcher suggested employing a thermal management system (TMS) to limit heat dissipation in monopolar electrosurgical operations, with positive results. To prevent thermal damage and tissue adhesion in minimally invasive surgery, the researcher employed ultrasonic vibration-assisted approach [12]. ESG should be studied and analyses in a realistic manner and tested on different loads, not just one, to verify the validity and strength of the improved methods used to improve its performance. Although the previous research focused on regulating the ESG's output power or reducing tissue thermal dissipation, their methods were not applied to the generator in its non-ideal state, as there are no electronic circuits that work perfectly 100% of the time. Additionally, the results were validated using a single load model. The load, on the other hand, is changeable due to the fact that important tissues vary in terms of tissue density, age, and sex. In [13], the researchers studied and examined the buck converter circuit, which is one of the device's electronic circuits in a non-ideal state. Tests on the examined circuit demonstrated that its behavior at 100 kHz is better from an economic and practical standpoint. Similarly, three different age and gender loads (child, male, and female) were explored as test models for the generator design process. This research provided a more in-depth analysis of the generator design process, but it provided no feasible ways to increase the generator's performance, as the data showed that output power changes with each of the three loads, as well as did not contribute to reducing heat dissipation.

This paper aims to develop and build an ESG that is more realistic and avoids the majority of possible issues. This study relies on research [13] in designing the ESG with a switching frequency of 500 kHz, as well as on the three loads considered, which include different layers for children, males, and female's tissues. The ESG's

output power is regulated using the standard IO-PID and FO-PID controllers as well as using optimal IO-PID and FO-PID controller's parameters. The ESG's output voltage and current waveforms are improved by replacing the three-level typical inverters with a five-level advanced inverter, which reduces or eliminates tissue thermal dissipation.

**Methods**

The closed-loop control system of ESG is designed in this work employing controllers of integer order PID (IO-PID) and fractional order PID (FO-PID). The particle swarm optimization (PSO) technique is then used to fine-tune the settings of each controller type in order to obtain the best values for the parameters that control the ESG's output power. In addition, to reduce heat dissipation, an advanced 5 multilevel inverter circuit was employed instead of the traditional H-bridge inverter circuit used in most research to design the ESG. The performance of the ESG is evaluated using a variety of control modes and inverter circuits, which are proposed in this paper.

Effect Temperature on the Tissue

The typical body temperature is approximately 37°C and may exceed 40°C. At these temperatures, the cellular structure of tissues is good. When the temperature is increased to between 60 and 100°C, the proteins solidify, resulting in the formation of clots and hence the coagulation process. When temperatures are above 100°C, the fluid inside the cells boils, causing the cell walls to break; this is referred to as the cutting process. Concerning the highest temperatures, this could result in the breakdown of organic molecules, resulting in what is known as carbonation [14,15]. Temperature increases beyond a predetermined threshold cause cellular damage to tissues [16,17]. Additionally, thermal diffusion caused by elevated temperatures can cause injury to adjacent organs such as the bladder, ureters, and intestines [18]. It's worth noting that around 4000 people every year suffer burns produced by electrosurgery, and 70% of these injuries are not noticed during surgery, but rather afterward, resulting in illness or death. This adverse effect is not confined to the patient, but also to the medical team, as substantial financial compensation is provided for such injuries [19,20]. Figure 1 displays some of the damage done by the ESG. The amount of thermal energy generated in biological tissues during electrosurgery can be calculated based on Joule's law of energy [14,21,22], which states that:

(1) $$Q = P \times t$$

where P can be written as:

(2) $$P = V \times I$$

where:
*Q* - is energy heat in joule (*J*)
*P* - is the output power in watt (*W*)
t - is the time interval for current to flow in second (Sec)
*V* - is the output voltage in volt (*V*)
*I* - is the output current in ampere (*A*).

According to the preceding two formulas, the amount of heat energy relies on the voltage, current, power, and time, also, the output power of the ESG is voltage and current dependent. As a result, it is possible to enhance the ESG's performance and reduce or eliminate thermal diffusion by controlling the ESG's output voltage and current. This is accomplished by optimizing the inverter circuit utilized in the ESG's construction, which is responsible for the ESG's output.

(a) (b) (c)

Figure 1. Injuries caused by the heat dissipation in electrosurgery. *Source: (a) [23]; (b) [24]; (c) [10].*

Tissue Bioimpedance Models

The biological electrical impedance of tissues can be defined as a measure of the opposition shown by materials resisting the flow of AC cur-rents at different frequencies and expressed physically by electrical impedance. This impedance reflects the clinical condition of the tissues re-quired for the clinical procedure [23]. The biological impedance can be calculated by Eq. 3 [24].

(3)
$$Z_{Tissue} = \frac{1}{\frac{1}{R_p} + \frac{j}{X_c}}$$

where:

$Z_{Tissue}$ - is bioimpedance of tissue in Ω

$R_p$ - represents water and electrolyte fluids resistance in the extracellular

$X_c$ - is capacitive reactance in Ω.

Inverter Circuit

An inverter is an electrical circuit that converts direct current to alternating current at the desired output voltage and frequency. However, the inverter circuit suffers from significant conversion losses and operates at a low practical efficiency [25]. The traditional inverter circuit generates square-shaped output voltage and current waves. This type of wave contains a significant proportion of total harmonic distortion (THD), which is undesirable in electrical circuits because it causes distortions in the current and voltage waveforms, as well as an increase in temperature and loss [26,27]. To overcome these issues, a multi-level inverter can be utilized to improve both the voltage and current waveforms, as well as the THD [25,28,29]. Figure 2 shows the H-bridge conventional inverter circuit, whose design and implementation were studied in the research [13]. Figure 3 shows the advanced 5 multilevel inverter circuit that is proposed in this study. The Fourier series method is used to calculate the ratio THD of the output for each type of inverter circuits.

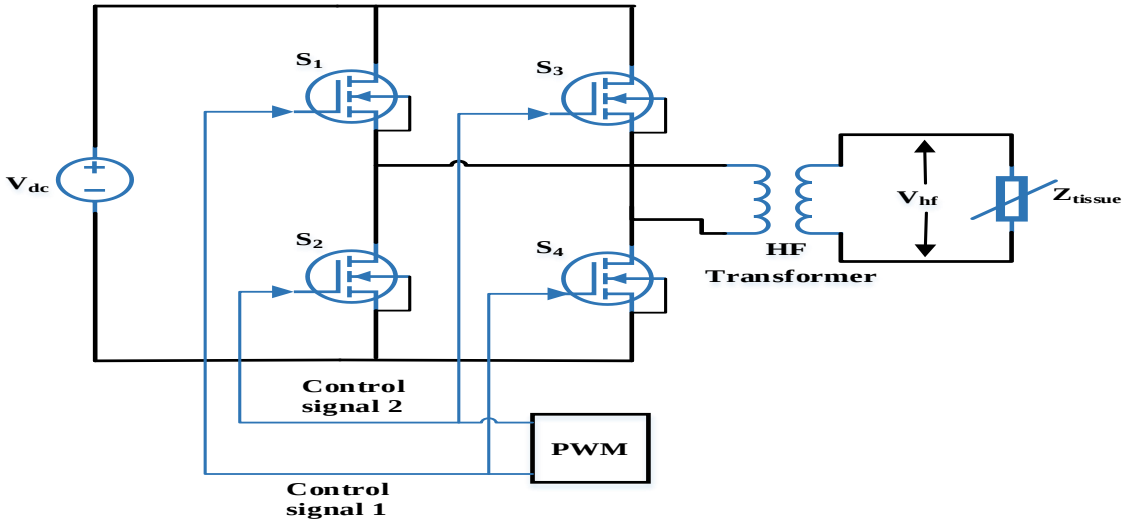


Figure 2. H-bridge conventional inverter circuit. *Source: [13].*

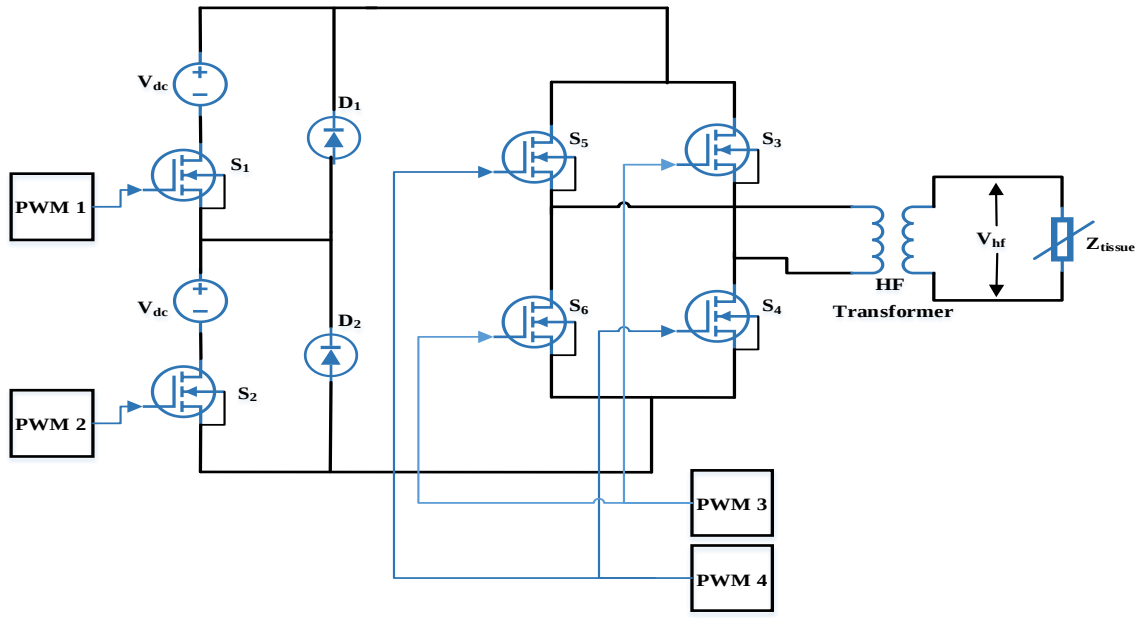


Figure 3. Advanced 5 multilevel inverter circuit. *Source: Authors.*

Total Harmonic Distortion (THD)

Based on Fourier series equation shown in Eq. a, THD of the output voltage and current for the conventional H-bridge and advanced inverter circuits of the ESG can be determined as follows :

(4) $$V_{HF}(Z_{Tissue}, nwt) = \frac{a_\circ}{2} + \sum_{n=1,2,3,\ldots}^{\infty} a_n \cos(nwt) + b_n \sin(nwt)$$

- Qualitative analysis for THD in case H-bridge inverter circuit

(5) $$a_\circ = \frac{2}{T}\int_0^T V_{HF}(Z_{Tissue}, nwt)dwt\,, a_\circ = 0$$

(6) $$a_n = \frac{2}{T}\int_0^T V_{HF}(Z_{Tissue}, nwt)\cos(nwt)\,dwt,\ a_n = 0$$

(7) $$b_n = \frac{2}{T}\int_0^T V_{HF}(Z_{Tissue}, nwt)\sin(nwt)\,dwt,$$

when n is even then bn = 0 and when n is odd bn is

(8) $$b_n = \frac{4V_{dc}(Z_{Tissue})}{n\pi}$$

subsisting Eq. 5, 6, and 7 in Eq. 4

(9) $$V_{HF}(Z_{Tissue}, nwt) = \sum_{n=1,2,3,\ldots}^{\infty} V_n \sin(nwt)$$

(10) $$I_{HF}(Z_{Tissue}, nwt) = \sum_{n=1,2,3,\ldots}^{\infty} I_n \sin(nwt)$$

(11) $$V_n = \frac{4V_{dc}(Z_{Tissue})}{n\pi}$$

(12) $$I_n = \frac{V_n}{(Z_{Tissue})_n}$$

(13) $$THD_v = \frac{\sqrt{\sum_{n=2}^{\infty}(V_{n,rms})^2}}{V_{1,rms}}$$

(14) $$THD_i = \frac{\sqrt{\sum_{n=2}^{\infty}(I_{n,rms})^2}}{I_{1,rms}}$$

- Qualitative analysis for THD in case advanced inverter circuit

(15) $$a_\circ = \frac{8}{T}\left[\int_{\alpha_1}^{\pi-\alpha_1} V_{HF}(Z_{Tissue}, nwt)dwt\right] + \frac{4}{T}\left[\int_{\alpha_2}^{\pi-\alpha_2} V_{HF}(Z_{Tissue}, nwt)dwt\right], a_\circ = 0$$

(16) $$a_n = \frac{8}{T}\left[\int_{\alpha_1}^{\pi-\alpha_1} V_{HF}(Z_{Tissue}, nwt)\cos(nwt)\,dwt\right] + \frac{4}{T}\left[\int_{\alpha_2}^{\pi-\alpha_2} V_{HF}(Z_{Tissue}, nwt)\cos(nwt)\,dwt\right], a_n = 0$$

(17) $$b_n = \frac{8}{T}\left[\int_{\alpha_1}^{\pi-\alpha_1} V_{HF}(Z_{Tissue}, nwt)\sin(nwt)\,dwt\right] + \frac{4}{T}\left[\int_{\alpha_2}^{\pi-\alpha_2} V_{HF}(Z_{Tissue}, nwt)\sin(nwt)\,dwt\right]$$

when n is even then $b_n = 0$ and when n is odd $b_n$ is

(18) $$b_n = \frac{4V_{dc}(Z_{Tissue})}{n\pi}[\cos(n\alpha_1) + \cos(n\alpha_2)]$$

subsisting Eq. 14, 15, and 16 in Eq. 4

(19) $$V_{HF}(Z_{Tissue}, wt) = \sum_{n=1,2,3,\ldots}^{\infty} V_n \sin(nwt)$$

(20) $$I_{HF}(Z_{Tissue}, nwt) = \sum_{n=1,2,3,\ldots}^{\infty} I_n \sin(nwt)$$

where:
$a_n$ and $b_n$ - are Fourier series components
n - is the number of orders for the harmonics
$V_{dc}$, $V_{HF}$; $I_{HF}$ and $Z_{Tissue}$ - are the DC input voltage
high-frequency AC output voltage
high-frequency AC output current and impedance tissue respectively
$THD_v$ and $THD_i$ - are the total harmonic distortion of the output voltage and output current respectively
$\alpha_1$ and $\alpha_2$ - are firing angles

**PID Controllers**

A fractional PID controller is a type of PID controller that is an extension of the conventional PID controller. The fractional order controllers are less sensitive to changes in the controlled system's and controller's characteristics. In ESG, an accurate control system is built using an integer order-PID (IO-PID) controller and a fractional order-PID (FO-PID) controller. IO-PID controller consists of three types of control i.e., Proportional, Integral, and Derivative control. FO-PID controller has two extra parameters, λ, and μ (orders of integration and differentiation), which make the controller more adaptable. Figure 4 shows a block diagram for the two controllers. The system transfer function in the continuous s-domain for IO-PID and FO-PID are given in Eq.20 and Eq.21 respectively, where Kp is the proportional gain, Ki is the integration coefficient and Kd is the derivative coefficient, λ and μ are the orders of integration and differentiation respectively [30,31].

(21) $$G_{IO-PID}(S) = K_p + \frac{K_i}{S} + K_d S$$

(22) $$G_{FO-PID}(S) = K_p(1 + \frac{K_i}{S^\lambda} + K_d S^\mu)$$

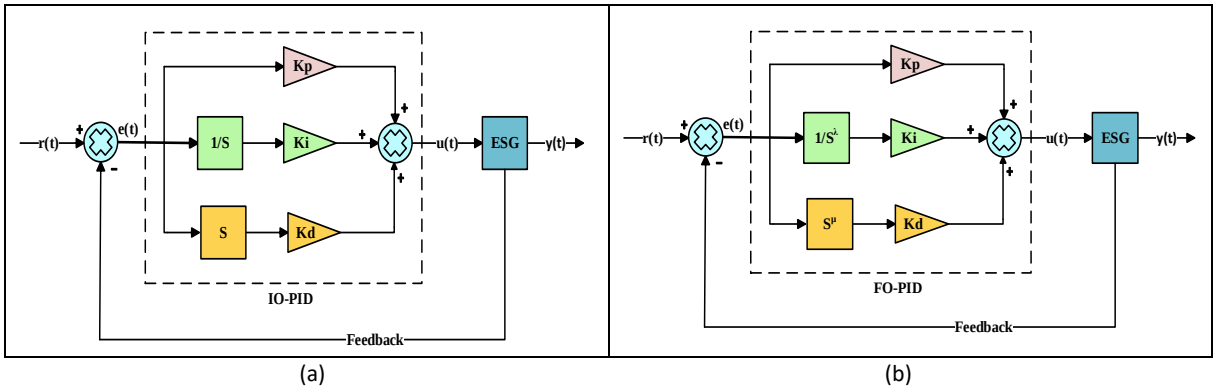


Figure 4. (a) IO-PID controller, and (b) FO-PID controller. *Source: Authors.*

The conventional particle swarm optimization (PSO) algorithm is used to adjust the parameters of each of the two types of controllers to get the best values for the parameters to achieve the desired goal. Figure 5 shows the block diagram of the IO-PID and FO-PID controllers with the PSO algorithm. It is worth noting, that the control system of both types of IO-PID and FOPID is applied to the two ESG, i.e., the ESG that is designed using the H-bridge traditional inverter circuit and the generator that is designed using the advanced 5 multilevel inverter circuit, to regulate the output power of each generator and watch the behavior of each type of the two generators and the affected of their practical properties.

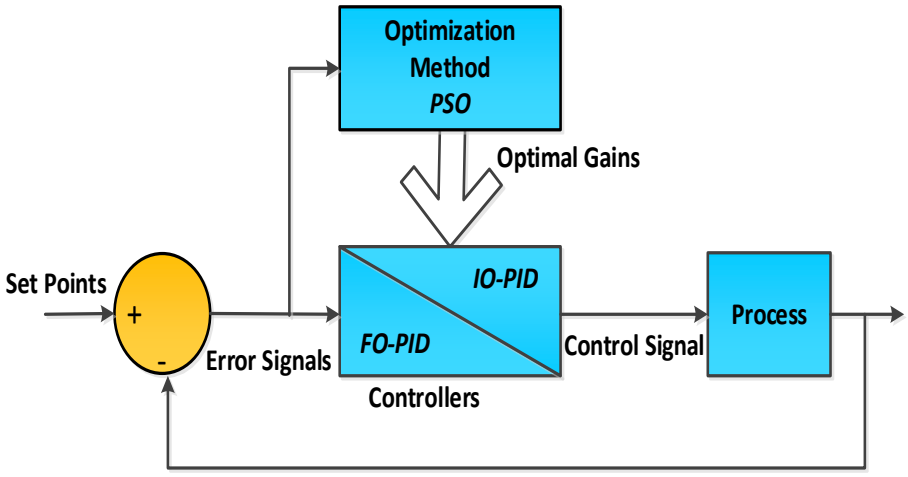


Figure 5. Block diagram of the PSO with IO-PID and FO-PID controllers. *Source: Authors.*

**Results and discussion**

The design and implementation of the ESG is done by MATLAB/SIMULINK environment. In this study, must be put two practical steps for the design process in order to reduce or eliminate the defects faced by the ESG, the most important of which is the irregularity of the output power to the ESG due to the nature of the variable impedance of the tissues, as well as the heat dissipation that occurs when performing the surgery, which causes burns or other side effects for the patient. The following are the first and second steps in the design procedure: In a closed-loop architecture, the ESG's output power can be controlled by a control unit even if the tissue impedance changes. To avoid harming the patient or medical staff, calculate the ESG's thermal energy output and, if necessary, lower it to a level that is safe for the patient. As IO-PID and FO-PID control units were used in this study, their performance was compared to see which type of controller performed best to improve the ESG's performance. The PSO algorithm was used to find the best values for controller parameters IO-PID and FO-PID. The control system is designed in the ESG, whose design and implementation were studied in the research [13], where the generator is designed at a frequency of 500 kHz and the ESG's output power (the desired amount of power set by the surgeon) is set to around 100 W a reference value to compare to the measured value of the output power. Additionally, the ESG's performance is evaluated after it has been equipped with the control system under three different loads (child, male, and female). The simulation results

demonstrate the behavior of each control type for various layers of each load type. The OV and Ts of the ESG's output power signals are compared. After developing an ESG with a control mechanism for regulating the generator's output power. The second phase in the design process is to calculate the quantity of thermal energy generated by the generator in order to determine the effect of the various types of controllers employed in the generator. Furthermore, the controller's ability to regulate the ESG's output power is considered. Thermal energy is computed for each of the layers using Eq. 1 for the three loads in the transient situation. Additionally, the percentage of thermal reduction for each type of controller can be determined using Eq. 22.

(23) $$RH = \frac{Q_{IO-PID} - Q_{measured}}{Q_{IO-PID}} \times 100\%$$

where *RH* denotes the degree of heat reduction. $Q_{IO\text{-}PID}$ (in Joules) is the thermal energy for each layer when using an IO-PID controller. This value is used as a reference for comparing thermal energy values for various controller modes. $Q_{measured}$ (in Joules) represents the thermal energy for each layer in other controller modes, such as standard FO-PID and optimal IO-PID or FO-PID controller settings. When the heat reduction ratio was calculated, it was found to be extremely low in all types of controllers. Additionally, the THD was quite high. As a result, it was required to identify suitable solutions to this problem. One alternative is to replace the conventional H-bridge inverter circuit with an advanced five-level inverter circuit. The ESG is constructed using a five-level multilevel inverter circuit. The same control system technique was used to design the ESG, utilizing a typical inverter to manage the output power under the same load mode. The simulation results demonstrate a significant improvement in the waveform for both the voltage and current outputs. When an advanced 5 multilevel inverter circuit was employed to design the ESG, the ratio THD was significantly reduced. Figure 6 illustrates the waveforms for the ESG's output voltage and current when a traditional inverter and an advanced 5 multilayer inverter are utilized.

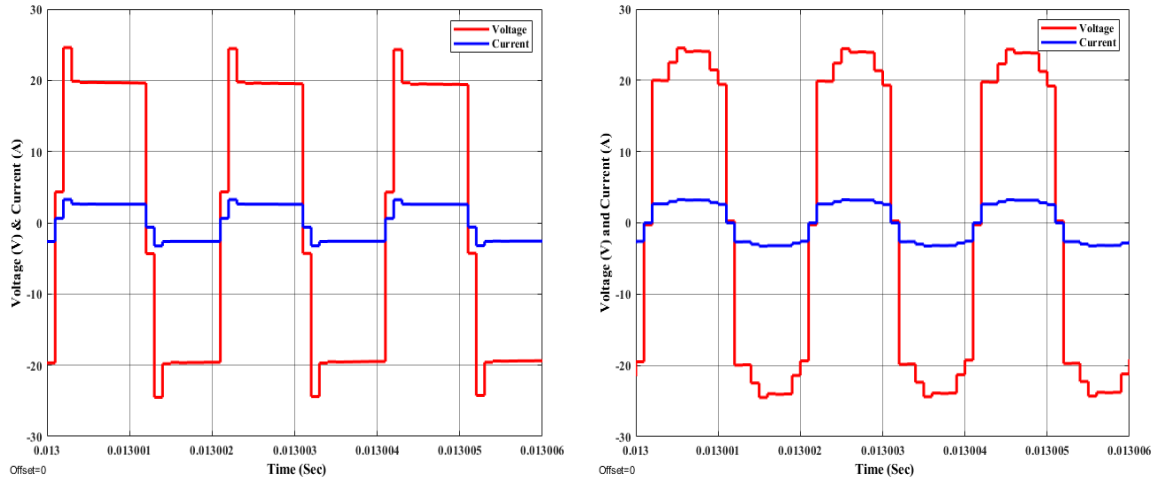


Figure 6. Output voltage and output current in 3 and 5 Level inverter circuit. *Source: Authors.*

In the case of employing PSO for tuning the parameters of FO-PID controller, Figure 7 illustrates the response of the output power of the ESG with traditional inverter circuit and the advanced 5 multilevel inverter circuit for the three load models. Tables 1, 2 and 3 show the comparison of the performance characteristics for the ESG, where Lxy represents type of layers (x: type for modes and y: type for layers). Four modes of control are used, considering overshot (OS (%)), and the percentage of reduction heat (↓RH (%)) for child, male, and female tissues. Additionally, two different types of inverters were used, including a conventional inverter and five multilayer inverters. Additionally, when a multilevel inverter is employed, the magnitude of overshot is reduced relative to when a traditional inverter is used. Furthermore, when compared to optimal IO-PID controllers, employing optimal FO-PID controller parameters in ESG can improve performance and decrease heat generation.

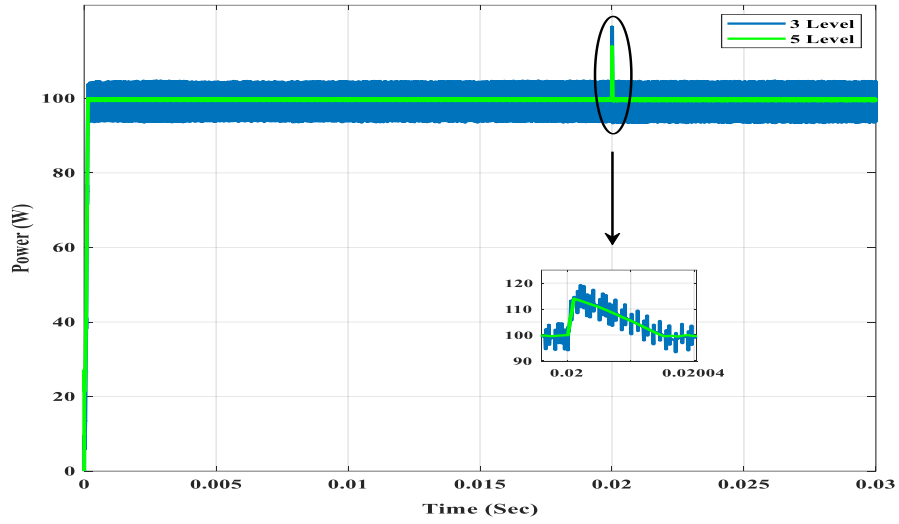


Child

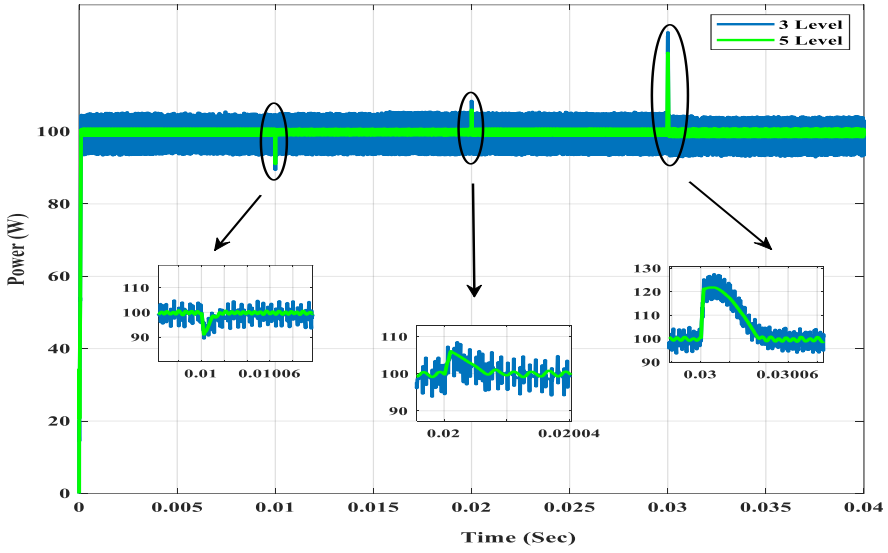


Male

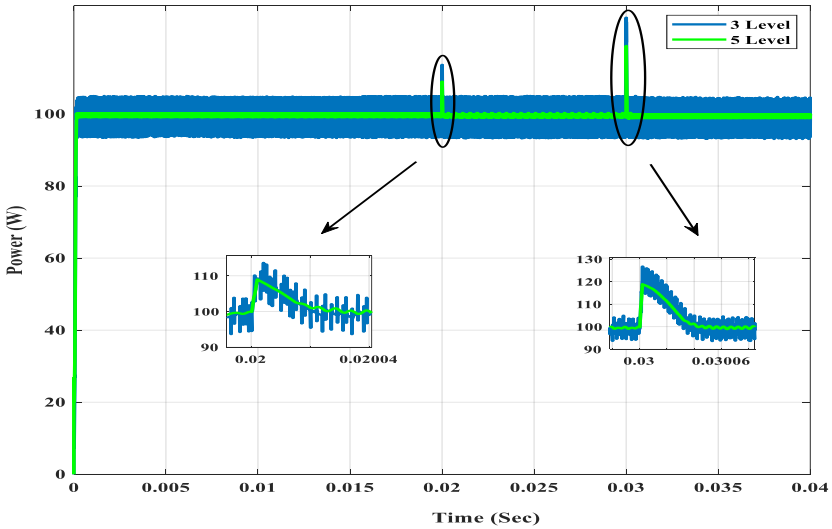


Female

Figure 7. Output power in 3 and 5 Level invert circuit for FO-PSO-PID of ESG. *Source: Authors.*

Table 1. Performance characteristics of ESG for case study child tissues. *Source: Authors.*

| Tissue Layer | Performance Factors | Symbol | PID Controller | | | |
|---|---|---|---|---|---|---|
| | | | IO | IO-PSO | FO | FO-PSO |
| $L_{11}$ | 3-Level Inverter | | | | | |
| | Overshoot | OS (%) | 19.62 | 10.50 | 5.09 | 4.28 |
| | Settling Time | Ts (μs) | 18.13 | 17.86 | 17.68 | 17.14 |
| | THD of current | $THD_i$ (%) | 41.36 | 41.36 | 41.34 | 41.34 |
| | Reduction Heat | RH (%) | 0 | 8.99 | 14.34 | 17.57 |
| | 5-Level Inverter | | | | | |
| | Overshoot | OS (%) | 12.13 | 3.91 | 0.43 | 0.04 |
| | Settling Time | Ts (μs) | 14.58 | 13.75 | 13.21 | 12.67 |
| | THD of current | $THD_i$ (%) | 21.69 | 21.69 | 21.67 | 21.67 |
| | Reduction Heat | RH (%) | 24.63 | 34.13 | 99.73 | 99.97 |
| $L_{12}$ | 3-Level Inverter | | | | | |
| | Overshoot | OS (%) | 5.55 | 5.14 | 4.56 | 4.45 |
| | Settling Time | Ts (μs) | 12.86 | 12.83 | 12.06 | 12.03 |
| | THD of current | $THD_i$ (%) | 41.36 | 41.36 | 41.34 | 41.34 |
| | Reduction Heat | RH (%) | 0 | 0.66 | 7.14 | 7.45 |
| | 5-Level Inverter | | | | | |
| | Overshoot | OS (%) | 0.89 | 0.82 | 0.17 | 0.02 |
| | Settling Time | Ts (μs) | 11.97 | 11.86 | 11.59 | 11.45 |
| | THD of current | $THD_i$ (%) | 21.69 | 21.69 | 21.67 | 21.67 |
| | Reduction Heat | RH (%) | 99.21 | 99.28 | 99.85 | 99.98 |
| $L_{13}$ | 3-Level Inverter | | | | | |
| | Overshoot | OS (%) | 26.69 | 25.03 | 23.24 | 19.47 |
| | Settling Time | Ts (μs) | 40.88 | 40.57 | 40.23 | 40.22 |
| | THD of current | $THD_i$ (%) | 41.36 | 41.36 | 41.34 | 41.34 |
| | Reduction Heat | RH (%) | 0 | 2.06 | 4.28 | 8.94 |
| | 5-Level Inverter | | | | | |
| | Overshoot | OS (%) | 21.54 | 21.38 | 19.96 | 13.98 |
| | Settling Time | Ts (μs) | 24.87 | 24.81 | 24.21 | 23.97 |
| | THD of current | $THD_i$ (%) | 21.69 | 21.69 | 21.67 | 21.67 |
| | Reduction Heat | RH (%) | 41.64 | 41.86 | 43.92 | 47.28 |

Impact of ESG

The power-controlled power of ESG units can have several positive impacts on surgical procedures, including:

- The ability to control the power output of electrosurgical devices, which allows surgeons to achieve more precise tissue cutting and coagulation, resulting in less tissue damage and a quicker healing time for the patient.
- By controlling the power of ESG units, surgeons can minimize the risk of unintended injuries or complications, such as burns, tissue damage, and hemorrhage.
- The precise cutting and coagulation capabilities of electrosurgical devices can reduce the time of surgery and operation, which leads to faster patient recovery and reduced healthcare costs.
- Controlled power of ESG units can reduce blood loss during surgery, which can be particularly important in procedures where blood loss is a concern.
- By minimizing the risk of unintended injuries and complications, controlled power of ESG units can enhance the safety of surgical procedures for both the patient and the surgical team.

Table 2. Performance characteristics of ESG for case study male tissues. *Source: Authors*

| **Tissue Layer** | **Performance Factors** | **Symbol** | **PID Controller** | | | |
|---|---|---|---|---|---|---|
| | | | **IO** | **IO-PSO** | **FO** | **FO-PSO** |
| $L_{21}$ | 3-Level Inverter | | | | | |
| | Overshoot | OS (%) | 8.31 | 5.26 | 5.22 | 4.67 |
| | Settling Time | Ts (µs) | 13.03 | 12.83 | 12.48 | 12.20 |
| | THD of current | $THD_i$ (%) | 41.53 | 41.53 | 41.52 | 41.52 |
| | Reduction Heat | RH (%) | 0 | 4.32 | 6.94 | 9.56 |
| | 5-Level Inverter | | | | | |
| | Overshoot | OS (%) | 4.50 | 2.42 | 0.71 | 0.62 |
| | Settling Time | Ts (µs) | 11.87 | 11.26 | 10.96 | 10.01 |
| | THD of current | $THD_i$ (%) | 18.84 | 18.84 | 18.84 | 18.84 |
| | Reduction Heat | RH (%) | 12.11 | 18.28 | 99.45 | 99.56 |
| $L_{22}$ | 3-Level Inverter | | | | | |
| | Overshoot | OS (%) | 7.09 | 4.69 | 4.35 | 4.00 |
| | Settling Time | Ts (µs) | 25.73 | 25.49 | 25.17 | 25.03 |
| | THD of current | $THD_i$ (%) | 41.53 | 41.53 | 41.52 | 41.52 |
| | Reduction Heat | RH (%) | 0 | 3.15 | 4.68 | 5.51 |
| | 5-Level Inverter | | | | | |
| | Overshoot | OS (%) | 2.09 | 1.39 | 0.73 | 0.64 |
| | Settling Time | Ts (µs) | 17.53 | 17.46 | 16.76 | 16.21 |
| | THD of current | $THD_i$ (%) | 18.84 | 18.84 | 18.84 | 18.84 |
| | Reduction Heat | RH (%) | 35.06 | 35.78 | 99.55 | 99.62 |
| $L_{23}$ | 3-Level Inverter | | | | | |
| | Overshoot | OS (%) | 17.35 | 15.31 | 13.92 | 9.87 |
| | Settling Time | Ts (µs) | 31.16 | 30.71 | 30.64 | 30.31 |
| | THD of current | $THD_i$ (%) | 41.53 | 41.53 | 41.52 | 41.52 |
| | Reduction Heat | RH (%) | 0 | 3.14 | 4.54 | 8.91 |
| | 5-Level Inverter | | | | | |
| | Overshoot | OS (%) | 10.87 | 10.34 | 8.37 | 6.04 |
| | Settling Time | Ts (µs) | 26.11 | 25.77 | 25.71 | 25.48 |
| | THD of current | $THD_i$ (%) | 18.84 | 18.84 | 18.84 | 18.84 |
| | Reduction Heat | RH (%) | 20.84 | 22.23 | 23.79 | 26.12 |
| $L_{24}$ | 3-Level Inverter | | | | | |
| | Overshoot | OS (%) | 40.12 | 36.03 | 34.94 | 28.76 |
| | Settling Time | Ts (µs) | 61.23 | 60.97 | 60.86 | 60.45 |
| | THD of current | $THD_i$ (%) | 41.53 | 41.53 | 41.52 | 41.52 |
| | Reduction Heat | RH (%) | 0 | 3.63 | 4.27 | 9.27 |
| | 5-Level Inverter | | | | | |
| | Overshoot | OS (%) | 30.50 | 30.46 | 29.79 | 21.75 |
| | Settling Time | Ts (µs) | 47.01 | 46.86 | 46.12 | 45.97 |
| | THD of current | $THD_i$ (%) | 18.84 | 18.84 | 18.84 | 18.84 |
| | Reduction Heat | RH (%) | 28.49 | 28.74 | 30.23 | 34.77 |

Table 3. Performance characteristics of ESG for case study female tissues. *Source: Authors.*

| Tissue Layer | Performance Factors | Symbol | PID Controller | | | |
|---|---|---|---|---|---|---|
| | | | IO | IO-PSO | FO | FO-PSO |
| $L_{31}$ | 3-Level Inverter | | | | | |
| | Overshoot | OS (%) | 16.03 | 5.69 | 5.11 | 4.62 |
| | Settling Time | Ts (µs) | 16.03 | 15.66 | 15.62 | 15.49 |
| | THD of current | $THD_i$ (%) | 40.79 | 40.79 | 40.78 | 40.78 |
| | Reduction Heat | RH (%) | 0 | 10.97 | 11.72 | 12.85 |
| | 5-Level Inverter | | | | | |
| | Overshoot | OS (%) | 9.12 | 5.02 | 0.45 | 0.11 |
| | Settling Time | Ts (µs) | 14.45 | 14.15 | 13.65 | 12.59 |
| | THD of current | $THD_i$ (%) | 18.55 | 18.55 | 18.55 | 18.55 |
| | Reduction Heat | RH (%) | 15.22 | 20.06 | 99.66 | 99.92 |
| $L_{32}$ | 3-Level Inverter | | | | | |
| | Overshoot | OS (%) | 8.57 | 6.72 | 6.65 | 4.58 |
| | Settling Time | Ts (µs) | 15.86 | 15.46 | 15.21 | 15.11 |
| | THD of current | $THD_i$ (%) | 40.79 | 40.79 | 40.78 | 40.78 |
| | Reduction Heat | RH (%) | 0 | 4.18 | 5.75 | 8.19 |
| | 5-Level Inverter | | | | | |
| | Overshoot | OS (%) | 2.90 | 2.18 | 1.53 | 0.29 |
| | Settling Time | Ts (µs) | 11.84 | 11.54 | 10.73 | 10.34 |
| | THD of current | $THD_i$ (%) | 18.55 | 18.55 | 18.55 | 18.55 |
| | Reduction Heat | RH (%) | 29.22 | 31.49 | 36.72 | 99.82 |
| $L_{33}$ | 3-Level Inverter | | | | | |
| | Overshoot | OS (%) | 20.16 | 18.55 | 16.92 | 13.73 |
| | Settling Time | Ts (µs) | 40.91 | 40.48 | 40.37 | 40.25 |
| | THD of current | $THD_i$ (%) | 40.79 | 40.79 | 40.78 | 40.78 |
| | Reduction Heat | RH (%) | 0 | 2.38 | 3.96 | 6.87 |
| | 5-Level Inverter | | | | | |
| | Overshoot | OS (%) | 13.78 | 13.34 | 12.62 | 8.96 |
| | Settling Time | Ts (µs) | 28.33 | 27.04 | 26.48 | 25.50 |
| | THD of current | $THD_i$ (%) | 18.55 | 18.55 | 18.55 | 18.55 |
| | Reduction Heat | RH (%) | 34.48 | 37.66 | 39.32 | 43.47 |
| $L_{34}$ | 3-Level Inverter | | | | | |
| | Overshoot | OS (%) | 33.29 | 32.33 | 31.47 | 26.74 |
| | Settling Time | Ts (µs) | 50.97 | 50.89 | 50.86 | 50.45 |
| | THD of current | $THD_i$ (%) | 40.79 | 40.79 | 40.78 | 40.78 |
| | Reduction Heat | RH (%) | 0 | 0.86 | 1.57 | 5.87 |
| | 5-Level Inverter | | | | | |
| | Overshoot | OS (%) | 26.50 | 26.09 | 25.02 | 18.87 |
| | Settling Time | Ts (µs) | 46.45 | 45.94 | 45.18 | 40.33 |
| | THD of current | $THD_i$ (%) | 18.55 | 18.55 | 18.55 | 18.55 |
| | Reduction Heat | RH (%) | 13.51 | 14.73 | 16.85 | 29.93 |

**Conclusions**

The conclusion of the research can be summarized as follows. A comprehensive study on power adjusting and heat dissipation in ESG units is demonstrated. The approach involved is implementing IO-PID and FO-PID controllers and optimizing their parameters using the conventional PSO algorithm. The typical H-bridge inverter is modified with an advanced five-level MLI to reduce heat dissipation and improve THD. The simulation results demonstrate that the FO-PID controller outperforms the IO-PID controller, especially when optimized using the PSO algorithm. This improvement is evident in the reduced overshot and settling times of the output power, as well as the significant decrease in heat dissipation. Moreover, the advanced five-level MLI is found to be more practical and efficient in reducing heat generation and THD compared to the typical H-bridge inverter.

The findings of this study have important implications for the design of ESG devices, which provide an effective method to mitigate the drawbacks of output power and heat dissipation. The optimal combination of FO-PID controller parameters and the advanced five-level MLI can be applied to other electrosurgical devices to achieve

better control of output power and heat dissipation. Future research will focus on developing an accurate thermal model of tissue to better understand the thermal behavior of tissue during surgery. The proposed heat equivalent circuit, as achieved in [32], will be used to demonstrate the heat transfer mechanisms between the tissue and ESG, providing insights into optimizing the performance of ESGs while maintaining patient safety.

**Conflict of interest**

The authors declare no conflict of interest.

**Acknowledgments**

The authors would like to thank and appreciate their universities for their support, which enabled the completion of this research.

**References**

[1] A. Eginli, W. Haidari, M. Farhangian, P.M. Williford, Electrosurgery in dermatology, Clin. Dermatol. 39 (2021) 573–579. https://doi.org/10.1016/j.clindermatol.2021.03.004.

[2] A. Ayesha, A. Nigam, A. Kaur, Principles of electrosurgery in Laparoscopy, Pan Asian J Obs Gyn. 2 (2019) 22–29.

[3] D. V. Belik, A. V. Shekalov, N.A. Dmitriyev, S.A. Bogavev, K. Dornhopf, Development of Radio-Frequency Electrosurgical Unit EHVCh-1.76, in: 2018 14th Int. Sci. Conf. Actual Probl. Electron. Instrum. Eng. APEIE 2018 - Proc., 2018: pp. 349–351. https://doi.org/10.1109/APEIE.2018.8545034.

[4] M.M. El-Sayed, E. Saridogan, Principles and safe use of electrosurgery in minimally invasive surgery, Gynecol. Pelvic Med. 4 (2021) 6–6. https://doi.org/10.21037/gpm-2020-pfd-10.

[5] I. Cordero, Electrosurgical units - How they work and how to use them safely, Community Eye Heal. J. 28 (2015) 15–16.

[6] T. V. Nechay, S.M. Titkova, M. V. Anurov, E. V. Mikhalchik, K.Y. Melnikov-Makarchyk, E.A. Ivanova, A.E. Tyagunov, A. Fingerhut, A. V. Sazhin, Thermal effects of monopolar electrosurgery detected by real-time infrared thermography: An experimental appendectomy study, BMC Surg. 20 (2020) 116. https://doi.org/10.1186/s12893-020-00735-6.

[7] S. Fahad, N. Ullah, A.J. Mahdi, N. Ullah, A new robust closed-loop control system for electrosurgical generators, Res. Biomed. Eng. 36 (2020) 213–224. https://doi.org/10.1007/s42600-020-00062-y.

[8] A.M. Ridha, A.J. Mahdi, J.K. Abed, S. Fahad, PID fuzzy control applied to an electrosurgical unit for power regulation, J. Electr. Bioimpedance. 11 (2020) 72–80. https://doi.org/10.2478/joeb-2020-0011.

[9] S. NasimUllah, M.M. Rafiq, M. Ishfaq, M. Ali, A. Ibeas, J. Herrera, A closed loop robust control system for electrosurgical generators, in: Control Appl. Biomed. Eng. Syst., Elsevier, 2020: pp. 149–168. https://doi.org/10.1016/B978-0-12-817461-6.00006-8.

[10] A.I. Abdullah, A. Yahya, M. Rava, T.T. Swee, N. Idris, Design and Developments of Thermal Control System of Electrosurgical Unit via Sensor Based on Thermometric Techniques, J. Phys. Conf. Ser. 1529 (2020) 042081. https://doi.org/10.1088/1742-6596/1529/4/042081.

[11] R.E. Dodde, J.S. Gee, J.D. Geiger, A.J. Shih, Monopolar electrosurgical thermal management for minimizing tissue damage, IEEE Trans. Biomed. Eng. 59 (2012) 167–173. https://doi.org/10.1109/TBME.2011.2168956.

[12] G. Yao, D. Zhang, D. Geng, L. Wang, Novel ultrasonic vibration-assisted electrosurgical cutting system for minimizing tissue adhesion and thermal injury, Mater. Des. 201 (2021) 109528. https://doi.org/10.1016/j.matdes.2021.109528.

[13] H.A. Saber, A.J. Mahdi, M.H. Nawir, S. Fahad, M.S. Nazir, A. Goudarzi, Investigation and testing of high-frequency open-loop electrosurgical generator under varying bio-tissue impedances, in: AIP Conf. Proc., 2022. https://doi.org/10.1063/5.0067040.

[14] V. Tomov, S. Tabakov, Modern Advances in Energy Based Electrosurgical Devices, (2018).

[15] D.E. Azagury, Book Review: The SAGES Manual on the Fundamental Use of Surgical Energy (FUSE), Springer, New York, 2013. https://doi.org/10.1177/1553350613483927.

[16] M. Ciesielski, J. Siedlecki, M.K. Janik, Mathematical modelling of thermal and electrical processes in the polyp-colon system during electrosurgical polypectomy, Int. J. Heat Technol. 38 (2020) 808–816. https://doi.org/10.18280/ijht.380406.

[17] J.S. Shim, Copyright Warning & Restrictions, 2007. http://scholar.google.com/scholar?hl=en&btnG=Search&q=intitle:Some+Contributions+on+MIMO+Radar#0.

[18] A. Karayiğit, İ.B. Karakaya, D.B. Özdemir, H. Dizen, İ. Özer, B. Ünal, Ü. Özdemir, Is electrosurgery

a revolution? Mechanism, benefits, complications, precautions, J. Pharm. Technolgy. 1 (2020) 60–64. https://doi.org/10.37662/jpt.2021.8.

[19] F.C. Meeuwsen, Safe Surgical Signatures, Delft University of Technology, 2019. https://doi.org/https://doi.org/10.4233/uuid:799ca1cd-d316-4919-8f0c-27f92db39ac5.

[20] M. El-Sayed, S. Mohamed, E. Saridogan, Safe use of electrosurgery in gynaecological laparoscopic surgery, Obstet. Gynaecol. 22 (2020) 9–20. https://doi.org/10.1111/tog.12620.

[21] H. Ferreira, C. Ferreira, Principle and Use of Electrosurgery in Laparoscopy, in: A Man. Minim. Invasive Gynecol. Surg., Jaypee Brothers Medical Publishers (P) Ltd., 2015: pp. 69–69. https://doi.org/10.5005/jp/books/12446_6.

[22] K. Charoenkwan, Z. Iheozor-Ejiofor, K. Rerkasem, E. Matovinovic, Scalpel versus electrosurgery for major abdominal incisions, Cochrane Database Syst. Rev. 2017 (2017). https://doi.org/10.1002/14651858.CD005987.pub3.

[23] U. Birgersson, Electrical impedance of human skin and tissue alterations: mathematical modeling, Karolinska Institutet, Sweden, 2012.

[24] K.R. Foster, H.C. Lukaski, Whole-body impedance - What does it measure?, Am. J. Clin. Nutr. 64 (1996) 388S-396S. https://doi.org/10.1093/ajcn/64.3.388s.

[25] S.H. Hosseini, A. Farakhor, S.K. Haghighian, New cascaded multilevel inverter topology with reduced number of switches and sources, ELECO 2013 - 8th Int. Conf. Electr. Electron. Eng. (2013) 97–101. https://doi.org/10.1109/eleco.2013.6713811.

[26] M.Z. Aihsan, N.I. Ahmad, W.A. Mustafa, N.A. Rahman, J.A. Soo, Development of square wave inverter using DC/DC boost converter, Int. J. Power Electron. Drive Syst. 10 (2019) 636. https://doi.org/10.11591/ijpeds.v10.i2.pp636-645.

[27] T. Dao, B.T. Phung, Effects of voltage harmonic on losses and temperature rise in distribution transformers, IET Gener. Transm. Distrib. 12 (2018) 347–354. https://doi.org/10.1049/iet-gtd.2017.0498.

[28] M. Salman, I.U. Haq, T. Ahmad, H. Ali, A. Qamar, A. Basit, M. Khan, J. Iqbal, Minimization of total harmonic distortions of cascaded H-bridge multilevel inverter by utilizing bio inspired AI algorithm, Eurasip J. Wirel. Commun. Netw. 2020 (2020) 66. https://doi.org/10.1186/s13638-020-01686-5.

[29] A. Y, Design and Simulation of Single-Phase Five-Level Symmetrical Cascaded H-Bridge Multilevel Inverter with Reduces Number of Switches, J. Electr. Electron. Syst. 07 (2018). https://doi.org/10.4172/2332-0796.1000281.

[30] K. Aseem, M.P. Subeekrishna, Comparitive Study of PID and Fractional Order PID Controllers for Industrial Applications, Int. J. Eng. Res. Technol. 7 (2019) 1–3.

[31] M. Dulău, A. Gligor, T.M. Dulău, Fractional Order Controllers Versus Integer Order Controllers, Procedia Eng. 181 (2017) 538–545. https://doi.org/10.1016/j.proeng.2017.02.431.

[32] G.M. Tina, W.H. Tang, A.J. Mahdi, Thermal parameter identification of photovoltaic module using genetic algorithm, in: IET Conf. Publ., IET, 2011: p. 21. https://doi.org/10.1049/cp.2011.0106.